A Design of PET detector using Microchannel Plate PMT with Transmission Line Readout

Heejong Kim, Chien-Min Kao, Henry Frisch, William W. Moses, Woon-Seng Choong, Jean-Francois Genat, Fukun Tang, Chin-Tu Chen

***Abstract*—A computer simulation study has been conducted to investigate the design of a PET detector module. The detector unit consisted of a 24x24 array of pixelated LSO crystals, each was 4x4x25 mm^3 in size, and two 102x102 mm^2 microchannel plate (MCP) PMTs coupled to both sides of scintillators. The crystal pitch was 4.25 mm and reflective media was inserted between crystals. The signals from MCP were readout using a transmission-line scheme. The optical photon inside scintillator was simulated by using the Geant4 package and the output signals of the MCP was formed by applying the electrical responses measured of the MCP to each individual detected photon. A experimental setup was built using a Photonis planacon MCP(XP85022) and a Transmission line board to measure the characteristics of MCP/TL. The measured single photoelectron response(SER) was fed to the simulation of the electrical signal. The responses to 511 keV gamma of the test setup were compared to the simulation results for the validation. The simulation study results showed an energy resolution of$\sim$11% at 511 keV for the detector module. When using a 400-600 keV energy window, we obtained a coincidence timing resolution of $\sim$323 ps FWHM and a coincidence detection efficiency of $\sim$40% for normally incident 511 keV photons. The position resolution was measured to be $\sim$4.25 mm. The readout at both ends of scintillator made it possible to infer depth of interaction(DOI) based on the energy asymmetry and time differences. The simulation study showed that the design is suitable for Time of Flight(TOF) PET with DOI capability.**

I. Introduction

MICROCHANNEL plate (MCP) photomultiplier tube (PMT) [1] is a promising photodetector for PET application due to its excellent positioning accuracy, fast time response, and compactness in comparison with the conventional PMT. Currently ideas for building large-area MCP PMT(e.g, 8x8 inch^2) cost effectively have been presented and are under investigation at the University of Chicago and Argonne National Laboratory [2]. Once the large area MCP PMT is realized, it would be a good alternative photodetector to replace the conventional PMT and make various PET detector designs possible.

We investigated a PET detector-module design that consisted of pixelated, thick LSO crystals and two MCP-PMTs. The high density and fast decay of the LSO, and the fast timing characteristics of the MCP-PMT, would make the module attractive for TOF PET imaging [3]. A transmission-line (TL) scheme [4] was employed for reading out the MCP-PMT outputs for estimating various event informations. This TL readout scheme can potentially allow us to extend the size of the detector module without substantially increasing the number of electronics detection channels. To extract DOI information, two MCP PMTs are coupled to LSO scintillators at both ends. The compact thickness of MCP makes this configuration feasible. The computer simulations were conducted to study the performance properties of this design. The optical photon's generation and transport were handled using Geant4 package. A experimental setup was built with a Photonis XP85022 MCP and TL board. The measured results were used as inputs to the design simulation. The comparisons between the experimental results and the simulation were done for the validation.

In Section II, the proposed detector configurations, readout scheme and Geant4 simulation setup are explained in detail. The experimental test setup and measured results are described in Section III. The results of the design simulation are shown in Section IV. The discussions and summary are in Section V.

Heejong Kim, Chien-Min Kao and Chin-Tu Chen are with the Department of Radiology, University of Chicago, IL, US

Henry Frisch, Jean-Francois Genat, Fukun Tang are with Enrico Fermi Institute, University of Chicago, IL, US

William W. Moses and Woon-Seng Choong are with Lawrence Berkeley National Laboratory, Berkeley, CA, US

II. Materials and Methods

A. Configuration

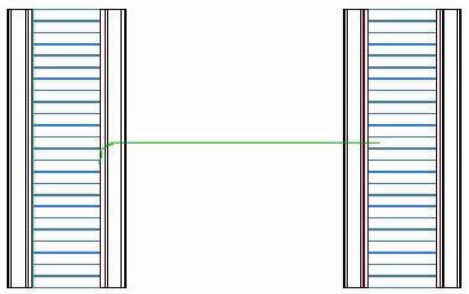

Fig. 1. Detector configuration with two modules. Each module consists of a 24x24 array of pixelated LSO scintillators and two MCP PMTs coupled to the scintillators at the front and back sides.

The detector configuration with two modules facing each other is shown in Fig. 1. One detector module consisted of 24x24 LSO pixels and two MCP PMTs that were coupled to the front and back sides of the scintillator array. For scintillator material, LSO was chosen due to its high light yield (30,000/MeV), fast decay($\sim$40ns), and high density. Each LSO pixel was 4x4x25 mm^3 in size and the crystal pitch was 4.25 mm. Photonis Planacon MCP PMT was used as a benchmark

9781-4244-3962-1/09/$25.00 ©2009 IEEE

in this study. Figure 2 shows a 2 inch Photonis Planacon MCP PMT (XP85022) [6] and a prototype transmission-line (TL) board that contains 32 strips. In the simulation study, we considered 102x102x9.1 mm^3 MCP PMT in order to match the size of the scintillator array. The TL board was assumed to have 24 strips with 4.25 mm pitch and these strips were considered as the anodes of the MCP PMT.

We have developed Geant4 [5] based codes to simulate the interactions of gamma rays with the detector, the generation and transport of the optical photons inside the scintillator array. The optical photon's behavior at the boundary surfaces was followed by the UNIFIED model. The surface of scintillator was treated as ground except the interface to the MCP, which was polished and treated with the optical grease for the higher light collection. The reflective media was inserted between the scintillator array. The detector responses to the coincidence event were obtained. For the coincidence event simulation, 511 keV gamma pairs were generated back-to-back to impinge on the centers of two modules. To study the uniformity of the detector-module response, different source positions were also considered.

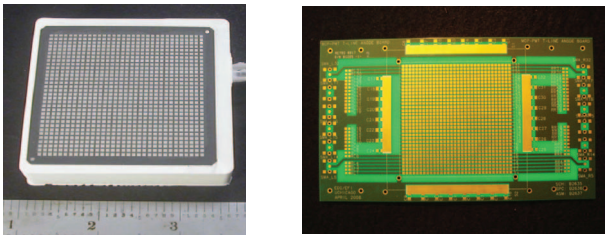

Fig. 2. Photonis Planacon MCP PMT (XP85022) with 1024 (32x32) anodes (left) and the prototype transmission-line board with 32 TL strips(right). One strip of TL makes contact with one row of MCP PMT anodes and signals are read out at both ends.

B. Signal forming and readout

Electrical signal was formed using Geant4 simulation outputs of the optical photon. Optical photon stops when it hits the photocathode of MCP PMT and the position and time at the photocathode are recorded. Photo-electron was generated depending on the wavelength and quantum efficiency of MCP PMT. The measured pulse shape with MCP/TL was assigned to each photo-electron. The observed signal at the TL are convolution of all photo-electron within the TL. Due to the gap between MCP layers and anode of the MCP PMT structure, the spread of the signal at anodes was observed larger than TL pitch(4.25 mm) and was handled by attributing $\sim$12% of the TL signal to the adjacent TLs. The gain variation and transit time spread were also taken into account in the convolution.

Fig. 3 depicts the TL readout scheme. The pulses in a TL propagate to both ends of the strip. We assumed that the waveform of the pulses are recorded with 10-20 GSps sampling, which was achieved using a digital oscilloscope for the real test. The energy can be obtained from the sum of two pulses and the average of two timing is regarded the event time. The interaction position is extracted from the centroid of TLs. Two MCPs readout makes the position determination

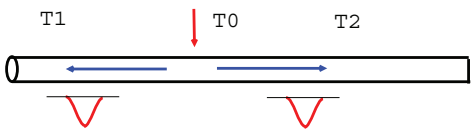

Fig. 3. Principle of Transmission-line readout. Two correlated pulses propagate toward the ends and are readout for energy and timing. By measuring the time difference, the interaction position along the TL can be inferred.

possible independently. The 24 strips in the forward MCP PMT run vertically to give x coordinate from the centroid. In the backward MCP PMT, the strips are rotated 90° with respect to the forward for y coordinate. In addition, the position information along the TL is available from the time difference measurement as follows.

$$X = \frac{\Delta T}{2} \times v \tag{1}$$

,where ΔT is the time difference $T1 - T2$ and v is the propagation speed of the signal on the TL. Compared to the individual crystal pixel readout, the TL scheme reduces the number of readout channel efficiently(from 576 to 48).

III. Experimental Tests

The test setup was built using a Photonis XP85022 MCP PMT and TL board. The main purpose of setup was to obtain the single photo-electron response of the MCP/TL. The simulation study can be more realistic by using the measured responses as inputs. The another aim is to measure the responses to 511 keV gamma. For this, the MCP/TL was coupled with LSO and an additional LSO/PMT was used for the coincidence setup. The real coincidence setup was also simulated separately and the measured results were compared with the simulation for validation.

Fig. 4 shows the assembled XP8500 MCP PMT on top of a TL board. XP85022 has two layer of Chevron type MCP with the pore diameter 10 μm. The prototype TL board has 32 micro strips with 1.6 mm pitch. Currently only 4 channels of TL can be readout with SMA type connectors. The waveform from the TL board was recorded by Tektronix DP07354 digital oscilloscope that samples the waveform with 10-20 GSps.

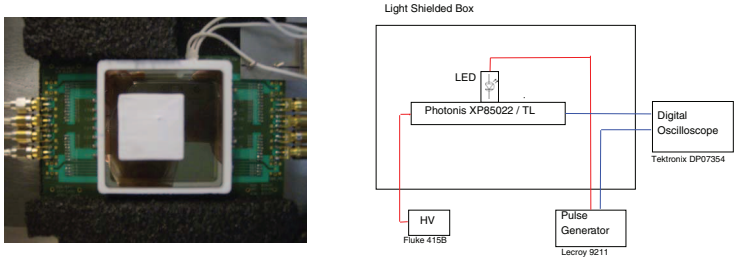

Fig. 4. Assembled XP85022 MCP/TL.(left) Four TLs at the middle have SMA type connectors for readout. A block diagram to measure SER with LED as a light source.

A. Single Photo-electron Responses

The setup to measure the SER of XP85022 MCP/TL is shown in a block diagram of Fig. 4. The LED(CMD204UWC-ND, CML Tech. Inc.) cased in cylindrical holder was placed on the MCP PMT. The light from the LED was localized through a 0.8 mm diameter aperture and was controlled by a pulse generator(Lecroy 9211) at single photon level. The high voltage(HV) for the XP85022 was set typically at -2300V. The waveform of three TL were recorded by the oscilloscope. The pulse shape of single p.e. is shown at Fig. 5. The rise time of SER was estimated ∼560 ps. The signal spread due to single p.e was larger than TL pitch and therefore the charge induced by single p.e, shown in Fig. 5, was obtained by integrating the pulses from three TLs.

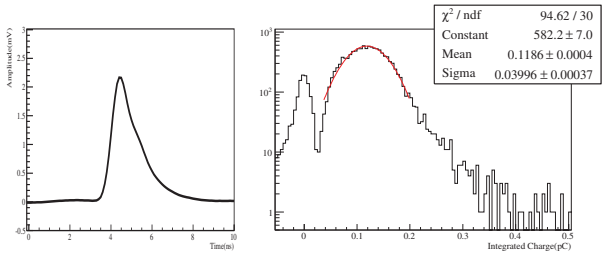

Fig. 5. Averaged pulse shape of single p.e(left) Only the middle TL was considered for the shape. Integrated charge distribution due to single p.e.(right) Due to single spread, charges of 3 TL pulses were summed together.

The absolute gain of XP85022 was measured from the integrated charge. By varying HV in -2100V and -2500V range, the gain as a function of HV was obtained as shown in Fig. 6 and was found well fitted by the exponential function as expected. The gain at -2300V, which was the nominal HV for the other tests, was $\sim 1.5 \times 10^6$. During the readout, only one side of TLs was used and the other was terminated with 50Ω. This was corrected by multiplying the factor 2 for the absolute gain.

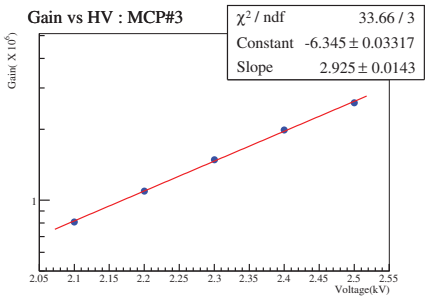

Fig. 6. XP85022 MCP gain as a function of HV. Each data point was calculated from the measured charge distribution.

B. Responses to 511 keV gamma

A LSO scintillator of 1x1x10 mm^3 was coupled to the XP85022 MCP/TL to measure the responses to 511 keV gamma. All the surfaces of the scintillator was polished. For a coincidence detector, another LSO of 6.25x6.25x25 mm^3 coupled to a Hamamatsu R9800 PMT was placed 3 cm apart.

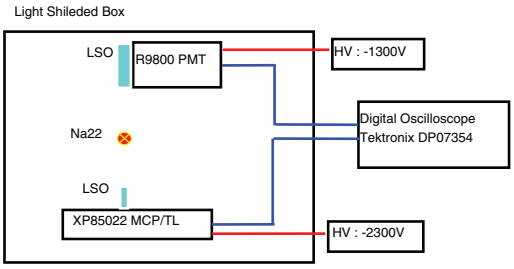

Fig. 7. Setup for 511 keV gamma coincidence event.

The long sides of two LSO scintillators are aligned to increase the coincidence rate. Na^{22} of ∼1 μCi activity was used as positron source at the middle of two units. The waveforms from three TLs and R9800 PMT were recorded by the digital oscilloscope. The coincidence event was triggered by requiring thresholds of 40 mV for the R9800 PMT and 8 mV for the MCP/TL, respectively. Fig. 7 shows the block diagram of the coincidence setup.

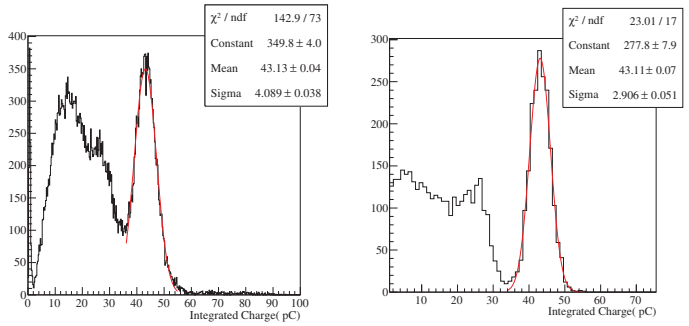

Fig. 8. Charge distribution of the MCP/TL from the experiment(left) and the simulation(right). Charges of the three TLs were summed. The unit was not not converted to the energy because the energy of 511 keV gamma was not fully confined in three TL according to the simulation.

The integrated charge distribution of the MCP/TL is shown in Fig. 8. Charge from the three TLs were summed in the figure. The peak corresponding to 511 keV and the compton continuum was seen clearly separated. The energy resolution at the peak was ∼22% in FWHM. In the same way, the charge distribution was obtained from the simulation of the coincidence setup for the comparison and shown in Fig. 8. In the simulation, the collection efficiency(C.E) was applied to reflect the ratio of open area inside the MCP in addition to Q.E. To make the peak value same as in the real test, the C.E was adjusted to 0.8 which was consistent with the measured separately. The resolution at the peak and shape of compton continuum shows differences between the real data and simulation. Simplified radioactive source distribution in the simulation might be one of the factor.

Fig. 9 shows the coincidence time distributions between the MCP/TL and R9800 PMT. Both for the real and simulation data, the timing was determined by the leading edge time pickup method by applying 3 mV and 50 mV thresholds for MCP/TL and R9800 PMT, respectively. To select the event around 511 keV peak, the charge was required to be

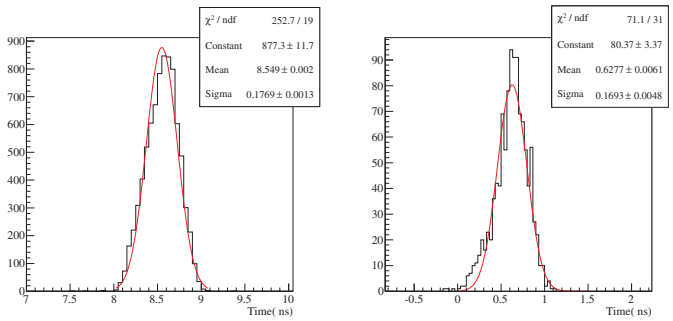

Fig. 9. Coincidence timing distributions: the experimental test(left) and the simulation(right).

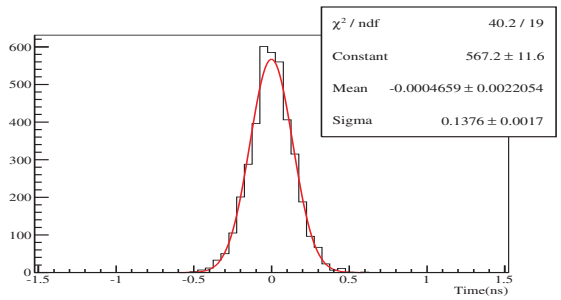

Fig. 11. Coincidence timing histogram. Event time in each module was determined by applying leading-edge pickup method, with 3 mV threshold, to the waveforms obtained at the maximum TL strip.

within [35, 60]pC range in Fig. 8. The measured coincidence timing resolution, ∼416 ps, was consistent with ∼398 ps from the simulation. The contribution from R9800 PMT on the coincidence timing was measured ∼200 ps from the coincidence setup using two identical LSO/R9800 PMT.

IV. Results : Design Simulation

The results shown in this section are obtained by analyzing 20K simulated events. In each event, two 511 keV gamma were injected to the central scintillator pixel of the detector whose coordinate was (2.125 mm, 2.125 mm) in XY. The positron range and accolinearlity were not considered in the gamma generation. The outputs of Geant4 detector simulation were combined to produce the signal pulses of the MCP/TL. The measured SER of the XP85022/TL (shown in Section III-A) was used for this. The gain variation of single p.e(80% FWHM) and the transit spread(80 ps FWHM) were taken into account for each photo electron.

A. Energy

To obtain event energy, the TL strip having the maximum signal was searched (called the *maximum TL strip* below) and then the signals of the five TL strips centered at the maximum TL strip were merged. The energy from the forward and backward MCP/TLs was summed for one detector module. Fig. 10 shows the resulting energy spectrum, which indicates a 11.0% (FWHM) energy resolution at 511 keV.

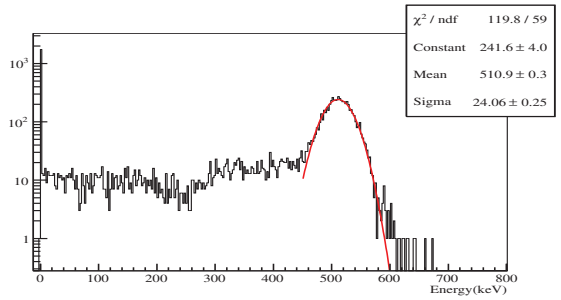

Fig. 10. Energy distribution of one detector module. The peak at zero energy corresponds to the events that pass the scintillator array without interaction. Fitting the photopeak with a Gaussian function indicates a 11% energy resolution at 511 keV.

B. Timing and Detection Efficiency

The event time was obtained by applying the LE time pickup method using 3 mV threshold to the waveforms obtained at the maximum TL strip. The measured timings at the forward and backward MCP/TL are averaged to reduce the effect of DOI on the timing determination. Figure 11 shows the coincidence timing histogram obtained by using a 400-600 keV energy window. The result shows ∼323 ps FWHM coincidence timing resolution. With this energy window, the detection efficiency for normally incident coincidence events was ∼40%: each module had a detection efficiency of ∼63%.

C. Position

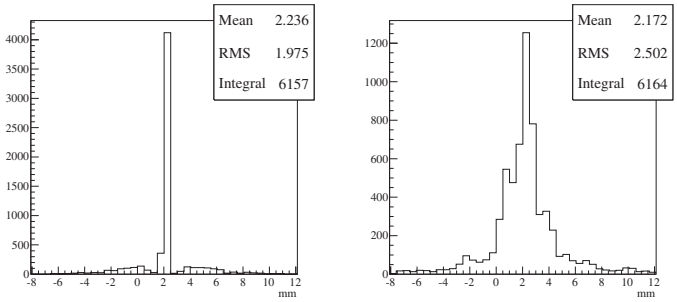

Fig. 12. The position reconstructed using the centroid(left) and the time difference on the TL(right).

The energy weighted centroid of the most energetic 5 TLs was taken as the interaction position. The coordinate in two dimension was calculated separately from the forward/backward MCP/TL. Fig. 12 shows a reconstructed X position distribution applying the centroid method on the forward MCP/TL signals. The energy window of [400, 600]keV was also required for the figure. Since the scintillator was pixelated all the way, the lights produced in a scintillator was highly localized and was reflected in the discrete pattern in the reconstructed position. The coordinate along the TL also determined based on the time difference at both ends of TL. Fig. 12(right) shows Y coordinate distribution calculated from the time difference of the highest energy TL using the Eq. 1. For the signal propagation speed of v, $c/3$ was used(c the speed of the light). The mean of the position was consistent with the result

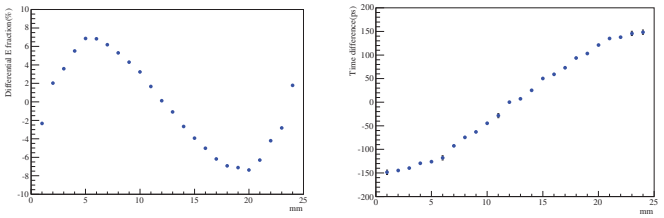

Fig. 13. Energy asymmetry (left) and time difference (right) between the signals at the front and back MCP-PMTs, as a function of the gamma injection position along the scintillator.

using the centroid method. The FWTM(Full Width at Tenth Maximum) of the distribution was comparable to 4.25 mm of the scintillator pitch.

D. Depth of Interaction

Signals obtained at the two MCP/TLs can be explored for obtaining the depth where a gamma photon interacts with the scintillator array [7]. We have investigated the correlations between the energy asymmetry and time difference between the signals obtained at the front and back MCP-PMTs with the depth of interaction (DOI). Energy asymmetry was defined as the ratio $(\mathrm{E_{front}} - \mathrm{E_{back}})/(\mathrm{E_{front}} + \mathrm{E_{back}})$, where $\mathrm{E_{front}}$ and $\mathrm{E_{back}}$ are the measured energy at the front and back MCP-MPTs. In this study, 511 keV gamma were injected from the side of scintillator array along the Z axis with 1 mm step. At each inject point, 20K events were generated for the simulation. Figure 13 shows the correlations of the energy asymmetry and time difference as a function of the gamma injection position along the Z axis. The linear correlation in time difference and the DOI was clearly seen. The S shape curve in the energy asymmetry might be effect due to the total internal reflection; when optical photons are generated closer to the ends of the scintillator the larger amount of light bounce to the other side at the boundary of LSO/MCP by total internal reflection. In addition to the correlation in time difference, exploiting of this distinctive feature would enhance the power to extract the DOI and is under investigation.

V. Discussion and Summary

We investigated the PET detector design adopting the MCP PMT and TL readout scheme. The detector consists of 24x24 LSO scintillator array coupled by two MCP/TLs at both sides. The simulation study based on Geant4 was conducted to evaluate the performance of the detector. The experimental tests was built using Photonis XP85022 MCP and prototype TL board and provided the SER for more realistic simulation. In our preliminary study, we obtained $\sim$11% energy resolution at 511 keV and $\sim$323 ps FWHM coincidence timing resolution while keeping $\sim$40% coincidence detection efficiency with a 400-600 keV energy window. The position resolution was $\sim$4.25 mm. The energy asymmetry and time difference of the signals, which are enabled from the feature of the detector, showed strong correlations with DOI. The simulation study showed that the design is suitable for TOF PET with the high sensitivity and the DOI capability.

The primary purpose of this study was to investigate the feasibility of the detector concept. Therefore, the optimization efforts enough to get the best performances has not been done yet and will be followed. The results reported here were obtained by using simple processing of the output signals. More advanced processing will be investigated to achieve better performance properties. For example, the signal waveforms at the TL can be sampled and digitally processed for producing more accurate arrival-time estimate (and more accurate positioning along the TL when estimated by using the arrival time difference) than the LE method [8]. It is also possible to analyze the spatial pattern of the TL signals for improving the estimates of the event position, timing, and DOI.

Acknowledgment

We would like to thank Greg Sellberg for the excellent soldering of XP85022 MCP and TL board and Mark Zaskowski for the various technical helps.

References

[1] J. L. Wiza, Nucl. Instr. and Meth. **162** (1979) 587-601.
[2] The Large Area Picosecond Photo-Detector Collaboration, http://hep.uchicago.edu/psec
[3] F. Bauer, M. Loope, M. Schmand, L. Eriksson, IEEE NSS/MIC Conference Record (2006) 2503-2505.
[4] J. Anderson, K. Byrum, G. Drake, C. Ertley, H. Frisch, J.-F. Genat, E. May, D. Salek, F. Tang, IEEE NSS/MIC Conference Record (2008) 2478-2481.
[5] S. Agostinelli et al., Nucl. Instr. and Meth. **A 506** (2003) 250-303.
[6] http://www.photonis.com
[7] J. S. Huber, W. W. Moses, M. S. Andreaco, O. Petterson, IEEE Trans. Nucl. Sci. **48**, (2001) 684-688.
[8] J.-F. Genat et al., Nucl. Instr. and Meth. **A 607** (2009) 387-393